arXiv:1611.06195v1 [cond-mat.quant-gas] 18 Nov 2016

Snake instability and the emanating vortex dynamics in two dimensional matter wave dark solitons

Gunjan Verma,[1] Umakant D. Rapol,[1,2] and Rejish Nath[1]

[1]*Indian Institute of Science Education and Research, Pune 411 008, India*

[2]*Center for Energy Sciences, Indian Institute of Science Education and Research, Dr. Homi Bhabha Road, Pune 411 008, India*

We analyze numerically the formation and the subsequent dynamics of two-dimensional matter wave dark solitons in a Thomas-Fermi rubidium condensate. An initially imprinted sharp phase gradient leads to the dynamical formation of a stationary soliton as well as very shallow grey solitons, whereas a smooth gradient only creates grey solitons. The depth and hence, the velocity of the soliton is provided by the spatial width of the phase gradient, and it also strongly influences the snake-instability dynamics of the two-dimensional solitons. The vortex dipoles stemming from the unstable soliton exhibit rich dynamics. Notably, the annihilation of a vortex dipole via a transient dark lump or a vortexonium state, the exchange of vortices between either a pair of vortex dipoles or a vortex dipole and a single vortex, and so on. For sufficiently large width of the initial phase gradient, the solitons may decay directly into vortexoniums instead of vortex pairs, and also the decay rate is augmented. Finally, we briefly discuss alternative techniques, they involve a Gaussian potential barrier in the presence of time-dependent interactions, both linear and periodic, to generate dark solitons, and the emerging dynamics. For the linear case, the soliton properties can be controlled by quench time. For the periodic modulation, a soliton lattice emerges and interestingly for sufficiently low barrier potential, both Faraday pattern and soliton lattice coexist.

I. INTRODUCTION

Dark solitons (DSs) are the most fundamental, localized nonlinear excitations appearing in various systems, [1–7] including Bose-Einstein condensates (BECs) [8–10], with defocusing non-linearity and they are characterized by a localized dip in the background density. Various techniques have been employed to generate matter wave DSs, for instance, phase imprinting [11–14], density engineering [15–17] and a combination of both, so called the quantum state engineering [18–21]. In addition, the formation of DSs has been reported for experiments, in which a condensate is flowing past an obstacle realized via laser induced dipole potential [22, 23], as well as during the interference of condensates initially prepared in multi-well potentials [24, 25]. DSs may also appear spontaneously in condensates, if the bose gas is quenched across the BEC phase transition via Kibble-Zureck mechanism [26–28]. Besides the experimental investigations, there has been numerous theoretical studies [29–34] discussing novel ways to generate, and study solitons, including their unique properties.

At zero temperatures, the stability of a DS demands a quasi one-dimensional condensate, i.e., the transverse extension of the condensate is required to be less than the healing length [35–38]. Otherwise, the soliton becomes dynamically unstable against transverse excitations, so called the snake instability (SI), which leads to the bending of the nodal stripe (plane) in a two-dimensional [39, 40] (three-dimensional) background, which eventually breaks up into vortices and sound excitations [41]. This has been observed experimentally in both matter wave [42] and optical DSs [43, 44]. At finite temperatures, thermodynamic instability may lead to the decay of dynamically stable DSs [45]. In the trapped case, even at zero temperature, DSs may exhibit dissipative losses due to the emission of sound waves and its repeated collisions with the latter [11, 46–48]. In general, the sound wave mediated dissipation of DS may occur if it encounters an inhomogeneity in the background density [49]. Non-conventional and exotic DS-like excitations are also predicted to exhibit in 2D condensates [40, 50, 51].

A dark stripe undergoing SI decays into a chain of vortices with opposite topological charges or the so-called vortex dipoles (VDs), a problem which has been addressed in the context of both non-linear optics [43, 44, 52–54] and in atomic condensates [40, 55–57], including fermionic superfluids [58]. If the transverse extension of the condensate is not large enough, the formed VD recombines back to form the dark stripe and will undergo SI again. This process keeps repeating in time [23, 55]. As the transverse size increases, more vortices are formed along the nodal stripe. Complementary to SI dynamics, it has also been shown that the various vortex configurations can be seen as the bifurcating states from a DS stripe [59]. The complex dynamics of vortices [60–62] including that of VDs [61, 63–75] in an inhomogeneous interacting condensate is a subject of its own merit. The motion of a vortex is strongly affected by the interaction with other vortices and the geometrical confinement. For instance, two vortices with same topological charge precess around each other, whereas with opposite charges move together with a linear velocity along the direction of flow between them. A VD may annihilate, [67, 73, 76–79] upon collision with other vortices or by emitting sound waves [80], a process that might play a big role in realizing the Onsager vortex states [81, 82].

In the first part of the paper, we numerically study the long-time dynamics of a 2D matter wave DS in a rubidium Thomas-Fermi (TF) condensate, subjected to SI. In particular, we look at the long-time dynamics of the VDs created. The DS is developed by imprinting a phase gradient at the start of the time evolution. The soliton properties, as well as the nature of SI and post instability dynamics, depend crucially on the spatial width of the phase gradient. A sharp phase variation at the centre of the condensate creates a stationary DS along with very shallow grey solitons, and the former eventually undergoes SI, results in a transient VD stripe. The stripe then breaks up into an interacting gas of VDs and lone vortices. The dynamics of vortices provides us very interesting scenarios: the

annihilation of a VD via an intermediate dark lump or vortexonium state, the collisional dynamics resulting in the exchange of vortices between either two VDs or a VD and a single vortex, etc. Interestingly, for the sufficiently large width of the initial phase gradient, the solitons may decay directly into vortexoniums instead of vortex pairs. In the final part, we briefly discuss alternative techniques to generate DSs in atomic condensates and the emerging dynamics. Especially, we focus on methods involving a Gaussian potential barrier and time-dependent interactions, both periodic and a linear quench. Interestingly, for the periodic case, a transient DS lattice emerges and depending on the height of the potential barrier it may coexist with Faraday patterns. The periodicity of the soliton lattice can be tuned easily by the modulation frequency.

The paper is structured as follows. In Sec. II we analyze numerically the SI dynamics of DSs in 2D TF condensates, in particular, the dependence of the spatial extension of the phase gradient. In Sec. III, we discuss the post-SI dynamics including that of the emanated VDs and vortexoniums. We discuss alternative techniques for generating DSs in Sec. IV, including how to control the soliton properties by tuning the system parameters. Finally, we conclude in Sec. V.

II. SNAKE INSTABILITY

DSs can appear as defects in the background density if we drive the initial state of the condensate into a dynamically unstable configuration. A simple way to achieve this is by imprinting a phase gradient in the condensate wave function, and in Sec. IV we discuss alternative techniques to achieve it. In this section, we focus mainly on the real-time dynamics of a 2D TF condensate with a phase gradient imprinted on it. We consider a BEC of N atoms confined in a harmonic trap: $V_t(\mathbf{r}) = m(\omega_x^2x^2 + \omega_y^2y^2 + \omega_z^2z^2)/2$ where ω_α is the trap frequency along the α axis. To simplify, we take $\omega_z \gg \omega_{x,y}$ such that the dynamics of the condensate along the z-axis is frozen and the system can be effectively described by a two-dimensional (2D) Gross-Pitaevski equation (GPE):

$$i\hbar\frac{\partial\psi(x,y,t)}{\partial t} = \left[\frac{-\hbar^2\nabla^2}{2m} + V_t(x,y) + g_{2D}|\psi(x,y,t)|^2\right]\psi(x,y,t), \tag{1}$$

where $\psi(x,y,t)$ describes the condensate wave function in the xy plane, $V_t(x,y)$ is the radial part of the harmonic confinement and $g_{2D} = g/\left(\sqrt{2\pi}l_z\right)$ is the effective coupling constant in 2D with $g = 4\pi\hbar^2aN/m$. The validity of Eq. 1 demands $l_z < \xi$ where $l_z = \sqrt{\hbar/m\omega_z}$ and ξ is the healing length [83]. We solve Eq. 1 in real time starting with the initial solution $\psi(x,y,t=0) = \psi_0(x,y)\exp[i\theta(x)]$, where $\psi_0(x,y)$ is the ground state solution of Eq. 1 obtained via imaginary time evolution and $\theta(x)$ is the $x-$dependent initial phase. By introducing a phase gradient along the x-axis, the dark solitons are generated with nodal lines parallel to the y-axis [11, 84]. First we take $\theta(x) = \pi/2$ for $x < 0$ and $\theta(x) = -\pi/2$ for $x \geq 0$, which introduces a sharp gradient at $x = 0$ with a phase difference of π. The resulting dynamics of the condensate is shown in Fig. 1(a)-(f). In the initial stage, a nodal stripe is developed [see, Fig. 1(a)] which eventually turns into a stationary DS at the centre of the BEC. The latter then undergoes SI [see, Fig. 1(b)], which leads to the formation of a transient stripe of VDs [see, Fig. 1(c)] and sound excitations [41, 42]. The SI has been attributed to the appearance of imaginary [36] or complex modes [41] in the Bogoliubov spectrum of a DS. In addition, we observe the formation of a large number of gray secondary solitons. There might be different sources associated with the formation of shallow solitons, for instance, shock waves are generated which shed DSs or the perturbations acting on the stationary DS [85]. Typically, very shallow DSs disintegrate quickly after hitting the boundary.

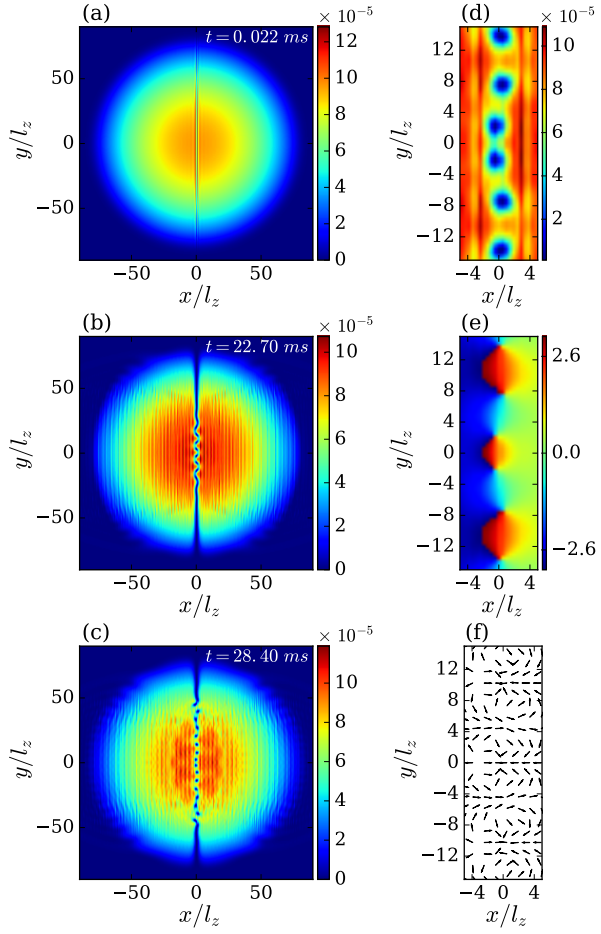


Figure 1. (Color online) The time evolution of the condensate density $n(x,y,t) = |\psi(x,y,t)|^2$ of a rubidium BEC with $N = 100$k, $a = 109a_0$, $\omega_x = \omega_y = 2\pi \times 10$ Hz and $\omega_z = 2\pi \times 700$ Hz, with an initial phase: $\theta(x) = \pi/2$ for $x < 0$ and $\theta(x) = -\pi/2$ for $x \geq 0$. (a) The condensate density at $t = 22\ \mu$s shows the formation a nodal stripe which eventually transforms into a stationary DS. (b) The SI first develops at the centre of the condensate. (c) A transient stripe of VDs emerge, and in (d) we show the VDs at the centre of the condensate. The phase and velocity fields corresponding to (d) are shown in (e) and (f) respectively.

Since the size of the condensate is much larger than the width (l_s) of the DS, we can describe the stationary soliton using the local density approximation (LDA)[86, 87].

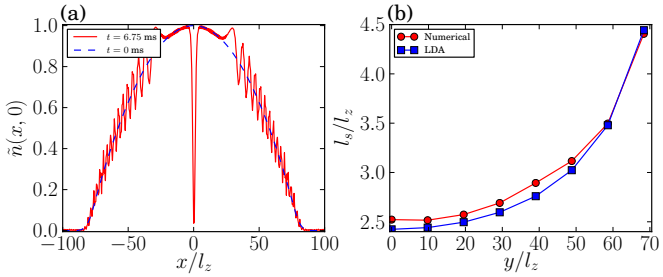


Figure 2. (a) The TF density profile $\left(|\psi(x, y = 0)|^2\right)$ at $t = 0$ (dashed line) and the emerged solitons at $t = 6.75$ ms (solid line). (b) The numerical results (filled circles) for the width $l_s(y)$ of the stationary DS as a function of y is compared with that of LDA with a TF profile (filled squares). The BEC setup is same as that of the Fig. 1.

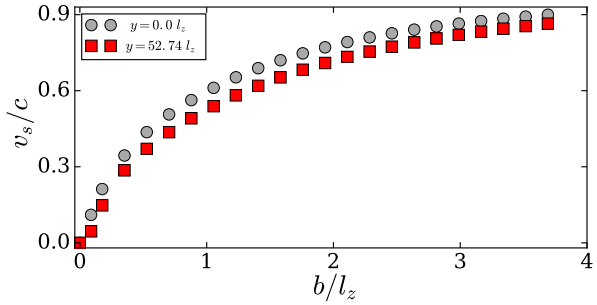


Figure 3. The subsonic local velocity v_s along the x-axis of the dark soliton as a function of b at different locations along the y-axis. For both curves, we calculated the velocity at $x = 1.5l_z$. At large values of b, v_s saturates to the speed of sound c, and also the centre of the soliton moves faster compared to the edges. The setup is same as that in Fig. 1.

The width l_s of a stationary DS in a homogeneous background is provided by the healing length ξ and is $\propto 1/\sqrt{n_h}$, where n_h is the uniform density of the condensate. Using the LDA, we can approximate the y-dependent width of DS as $l_s(y) = \hbar/\sqrt{mg_{2D}n_0(y)}$ calculated at $x = 0$, where $n_0(y) = |\psi_0(x = 0, y)|^2$. If we assume a Thomas-Fermi (TF) profile, the condensate density becomes $n_0(x, y) = \mu/g_{2D}\left[1 - x^2/R_x^2 - y^2/R_y^2\right]$ for $\{x \le R_x \ \& \ y \le R_y\}$ otherwise $n_0(x, y) = 0$ with $R_{x,y}^2 = 2\mu/\left(m\omega_{x,y}^2\right)$. As we move away from the centre towards the edge of the condensate l_s increases as a function of y since the density decreases. In Fig. 2, we compare the numerical results for l_s with that of LDA using TF profile. They are found to be in excellent agreement. For the numerical result, the l_s is calculated at an instant of time at which the nodal stripe has completely developed into a stationary soliton, and after which the width of the DS hardly changes before undergoing SI.

Further, we have noticed that the SI of DS develops first at the centre of the condensate [see Fig.1(b)] and later it spreads across the entire soliton. We explain this behaviour using LDA as follows. The SI in a homogeneous background is attributed to the imaginary low-momentum transverse excitations [36] as stated above. They appear for momenta $0 \le q\xi \le 1$ with a maximum value of $\mu_h/4$ at $q\xi = 1/\sqrt{2}$, where q is the quasi-momentum and $\mu_h = g_{2D}n_h$ is the chemical potential of the homogeneous density. The maximum imaginary mode provides us the growth rate and hence determines the time scale at which the SI develops, which is $\tau = 4/\mu_h$. Using LDA for the inhomogeneous case, we get $\tau(y) = 4/[g_{2D}n_0(y)]$, which indicates that the instability grows faster at the centre compared to that in the edge.

Smooth phase gradient: at this point, we replace the sharp phase gradient with a smooth one, $\theta(x) = (\pi/2)\tanh(x/b)$, which varies over a width b [29]. Interestingly, the characteristics, SI and post-SI dynamics of the DS depend crucially on the parameter b. Note that, $b = 0$ corresponds to the sharp gradient scenario discussed above and in that case, a stationary DS is created at the centre of the condensate. When b is nonzero, the phase becomes continuous at $x = 0$ and as expected, instead of a stationary soliton, a primary DS with a nonzero subsonic y dependent velocity $v_s(y) \approx c[1 - n_d/n_0(y)]^{1/2}$ along the x-axis is created, where $c = \sqrt{gn_0/m}$ is the speed of sound and n_d is the density depth of the DS. Since n_d decreases with increase in b, the velocity v_s increases, as shown in Fig. 3. At large values of b, the velocity v_s saturates to c [11]. The density dependence of the soliton velocity results in the bending of the nodal stripe during time evolution [see Fig. 4], which is unrelated to the SI dynamics.

The SI dynamics is also strongly modified by the parameter b. For small b, the instability process is analogous to that of the stationary case discussed above, in a way that the instability grows first at the centre of the soliton stripe, see Fig. 4(a), then progress to the rest of the stripe. In contrary, as b increases, the instability appears simultaneously at the centre as well as at the edges, leaving an intermediate fragment of DS unaffected. Hence, by the time SI develops in the intermediate region, the vortex dipoles are already created at the centre and the edges, see Fig. 4(b). If b is further augmented, the instability occurs first at the edges as shown in Fig. 4(c), then propagate towards the centre. Later, the entire soliton breaks up into VDs. Note that for sufficiently large values of b, very shallow solitons are formed with $v_s \sim c$ which dissipate before the SI develops.

III. VORTEX DYNAMICS

The extended time evolution of the phase imprinted condensate reveals very rich and interesting scenarios in the vortex dynamics, especially of VDs. A stationary DS breaks up into an unstable configuration of a stripe of VDs, which eventually disperses into a gas of interacting vortices and VDs. In course of time, we observe the following frequent events:

1. vortex pair annihilation, where two vortices of opposite charge approach each other, then coalesce into a dark lump [40, 88] or a vortexonium state [82] which subsequently decays by emitting sound waves. Vortexonium is characterized by a phase slip identical to that of a dark soliton, and it may revert to vortex dipole by hitting the

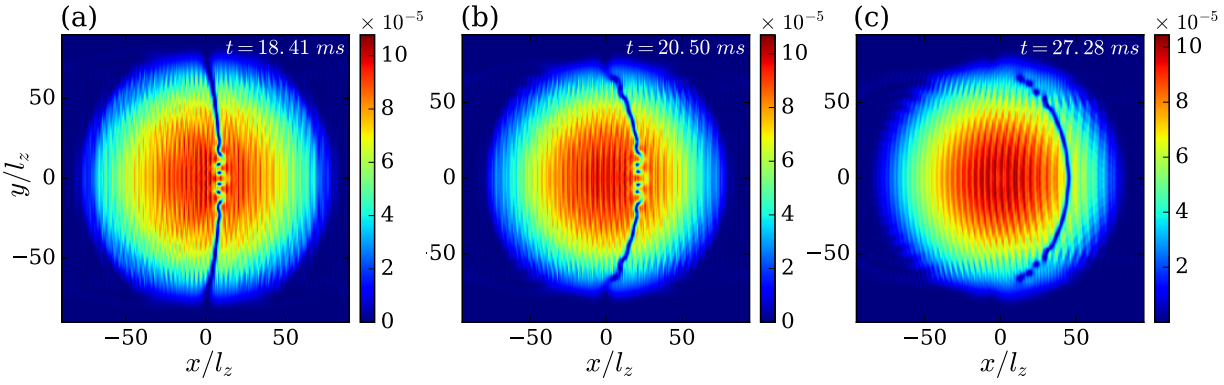


Figure 4. (Color online) The SI dynamics for different b is depicted through the condensate density $n(x, y, t) = |\psi(x, y, t)|^2$. (a) The SI develops first at the centre for $b = 0.05 l_z$. (b) The SI develops both at the centre and the edges simultaneously for intermediate value of $b = 0.2 l_z$. (c) For sufficiently large values of $b = 0.75 l_z$ the instability occurs first at the edges. In the later stage the whole DS breaks up into vortex dipoles. Note that, larger the b shallower the soliton is, hence faster it propagates. The setup is same as that in Fig. 1.

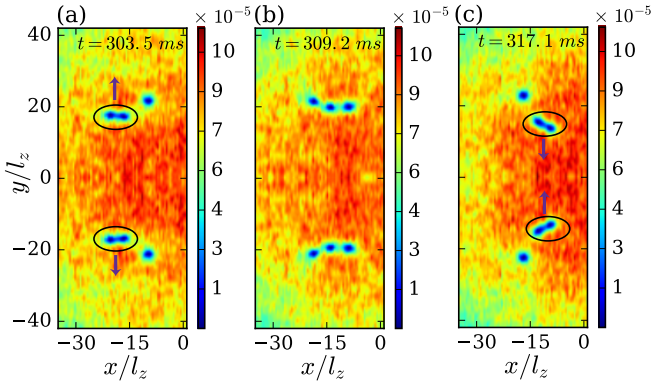


Figure 5. (Color online) (a) Two lone vortices are approached by two vortex dipoles and in (b) when they reach close to each other. In (c), an exchange of vortices has been taken place and a new pair of vortex dipoles are created. The setup is same as that in Fig. 1 with an initially imprinted sharp phase gradient. The initial and final VDs are indicated by ellipses and direction of propagation of VDs are shown by arrows.

boundary. VD annihilation has been reported in a BEC experiment [73], including in the context of superfluid turbulence [77]. The vortexonium may annihilate or decays to a smaller one, in the course of collision with a vortex or a VD. Also, we often noticed that the vortexoniums those propagate from the boundary towards the centre self-annihilate. Among vortexoniums we found two scattering events, in one case two of them collide with each other, then emerge out intact and move away [40]. In the second case, after the collision one decays while the other breaks up into a VD. It is difficult to pinpoint on what condition each of these processes occurs independently and may depend on the kinetic energy of the vertexoniums at the instance of collision.

2. A VD, after colliding with a lone vortex, form a new VD and a new single vortex [88, 89]. Two such process happening simultaneously are shown in Fig. 5. The nature of dynamics, either flyby or exchange processes, depends on the relative velocity and the impact distance between theVD and the single vortex [88]. While approaching the single vortex, the VD slows down (also the energy of VD increases) hence, undergoing structural modifications, in particular, the vortex-anti vortex separation increases. Finally the antivortex of the original VD merges with the single vortex forming a new VD, accompanied by radiative losses as sound excitations. The new VD propagates in a direction opposite to that of the initial one resulting in a *back scattering*.

3. A pair of VDs upon head to head collision, break up and exchange their partners, leading to the formation of a new pair of VDs, see Fig. 7. The new ones move perpendicular to the initial direction of propagation, as well as opposite to each other.

4. Two VDs approaching each other would either convert into two vortexoniums or annihilate one among them upon collision.

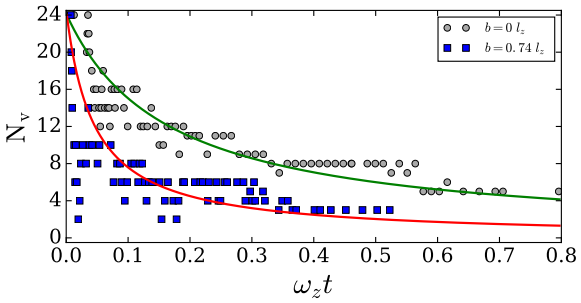


Figure 6. The number of vortices as a function of time for two different b. Larger the value of b, faster the decay of vortices. The solid lines are calculated using the rate equation given in Eq. 2 with $\Gamma(0) = 0.25$ and $\Gamma(0.74) = 0.9$. The oscillations in the vortex decay curve is due to the transitions between vortexoniums to VDs and vice versa. The setup is same as that in Fig. 1.

The parameter b indirectly influences the vortex dynamics. In particular, for sufficiently large b, the solitons first break from the edges into VDs, as mentioned above, then they quickly coalesce into vortexoniums. Finally, two adjacent vortexoniums collide, and one of them gets annihilated. This process repeats, resulting in the decline of the number of vortices as time progresses. We observed that as b increases the annihilation process is more frequent causing a faster decrement in vortex number, see Fig. 6. The oscillations in the vortex decay curve is due to the transitions between vortexoniums and VDs. The effective decay in the number of vortices, N_v, is well captured by the phenomenological rate equation [77],

$$\frac{dN_v}{dt} = -\Gamma(b)N_v^2, \tag{2}$$

where the decay coefficient $\Gamma(b)$ depends on b. The results according to the rate equation is shown as solid lines in Fig. 6. Another interesting feature we noticed is that, at sufficiently large b, DS travels faster, and breaks directly into vortexoniums at the boundary. This indicates that VDs are not necessarily the direct consequence of SI in 2D, depending on the nature of DS and its background density, it may break directly into vortexoniums.

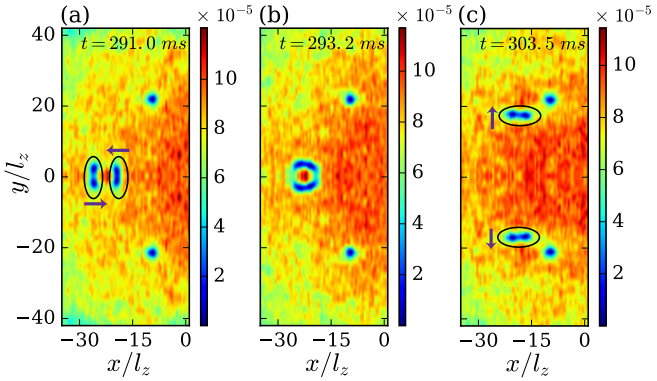


Figure 7. (Color online) (a) Collision of two counter propagating VDs. (b) Upon collision they exchange vortices and form a new pair of VDs. The new pairs propagate opposite to each other in a direction perpendicular to the axis of collision, as shown in (c). The initial and final VDs are indicated by ellipses and direction of propagation of VDs are shown by arrows.

IV. ALTERNATIVE TECHNIQUES FOR SOLITON GENERATION

In this section, we discuss alternative techniques for the generation of DSs in BECs and the corresponding dynamics in a 2D condensate. The methods involve the use of an external potential barrier and time-dependent interactions, $g_{2D}(t)$. A potential barrier can be induced by an optical dipole potential or a far-detuned laser field. Generation of 1D solitons due to the sudden removal of the potential barrier is theoretically studied in [19, 90], and is also experimentally demonstrated [16, 22, 23]. It has shown that the creation of DSs require the system to be in a non-linear regime where the interaction energy dominates the kinetic part [23, 91]. The characteristics of the solitons also depend crucially on the initial phase difference between the disconnected condensates, for instance, a phase difference of π may lead to the formation of a stationary soliton [91] accompanied by very shallow solitons, similar to that discussed in Sec. II. The number of solitons can also be controlled by fine tuning the initial separation between the condensates.

A. Gaussian barrier and time dependent interaction

We consider the same setup of BEC as in Sec. II with an additional Gaussian x-dependent potential barrier : $V_G(x) = V_0 \exp(-x^2/2d^2)$ of width d and height V_0, at the centre of the trap. Hence, effectively we have a double well potential along the x-axis. Now, introducing the time-dependent interaction leads to the dynamical formation of solitons. In other words, the nodal stripe which is not a DS created by the potential barrier acts as a source of DSs in the presence of $g_{2D}(t)$. Below, we consider both linear and periodic variation of g in time [92]. Note that, any non-zero V_0 breaks the radial symmetry of the condensate, and for sufficiently large V_0 and d, the condensate splits symmetrically into two disconnected BECs along the x-axis.

1. *Linear variation of g in time*

Here, we consider the linear variation of scattering length a in time t, such that

$$g_{2D}(t) = \begin{cases} g_{2D} + \delta g\ \alpha t, & 0 < \alpha t \leq 1 \\ g_{2D} + \delta g, & \alpha t > 1, \end{cases} \tag{3}$$

where δg is the difference and α is the rate at which g is varied over a time $\tau = 1/\alpha$. In the presence of the Gaussian barrier, $g(t)$ leads to the formation of DSs in the condensate [see Fig.8(a)]. The properties of the soliton depend on V_0, d, α and δg. Hence, by controlling these parameters, the DSs can be generated in a more controlled way. As we have found, both increment and decrement in g lead to the formation of solitons. If the ramping of $g(t)$ fulfills the adiabatic criteria [93, 94], the condensate adiabatically follows the instantaneous ground state, and as a result, no solitons are generated. This has two immediate consequences on the properties of DSs; as α decreases, for a fixed δg: (i) the number of solitons decreases and (ii) they get shallower and shallower [see Fig.8(b)]. On a similar note, for a fixed α, the soliton depth and also the number of solitons increases with increase in δg.

2. *g periodic in time*

In this section, we take $g_{2D}(t) = g_{2D}[1 + 2\alpha \sin(2\omega_m t)]$, where α and ω_m are respectively the amplitude and frequency of the modulation. As we show below, the numerical results

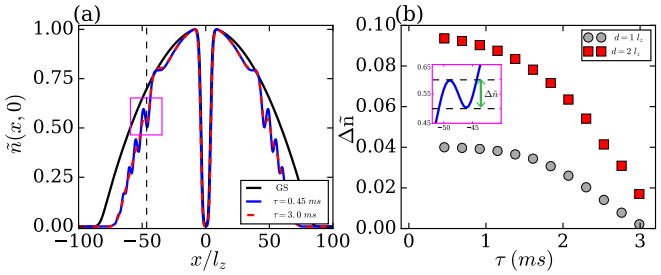


Figure 8. (a) The ground state (GS) profile $|\psi(x, y = 0)|^2$ (black solid line) and the emerged solitons for different ramp times, $\tau = 1/\alpha =$ 0.45ms (blue solid line) and $\tau =$ 3ms (red dashed line) are shown. All plots are renormalized with its corresponding maximum density and the snapshots are taken at different instants of time for different τ. (b) Relative soliton depth (filled circles) for the width $d = 1l_z$ and $d = 2l_z$ (filled squares) as a function τ is plotted. The soliton depths are calculated at the same location [$x = 46.5l_z$, shown with a box in (a)] in the condensate, shown by dashed vertical line in (a). The definition of $\Delta\tilde{n}$ is schematically shown in the inset of (b), which corresponds to the box in (a). The BEC setup is same as that of the Fig. 1, and for both (a) and (b) we take $\delta g = -g_{2D}/2$.

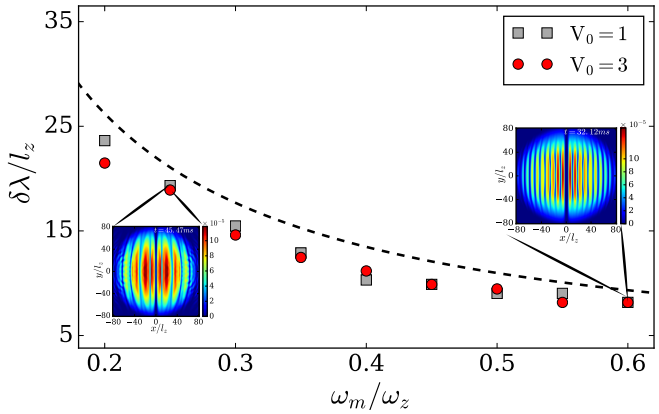


Figure 9. DS lattice periodicity vs modulation frequency, ω_m for $V_0 = 1$ (squares) and for $V_0 = 3$ (circles) with $\alpha = 0.2$ and $b = 0.86l_z$. The two insets show the density snapshots for $V_0 = 3$ at $\omega_m = 0.25$ and $\omega_m = 0.6$. The dashed line shows, $1/k = \epsilon^{-1}(\omega_m)$, the wavenumber corresponding to the Bogoliubov frequency ω_m.

for the dynamics of the system depend crucially on whether the initial state has a noise or not. In experimental setups always, there exist noise in the form of thermal or quantum fluctuations. They play an important role in, for instance, spontaneous symmetry breaking (SSB). A prime example for SSB is the formation of Faraday patterns in condensates by the parametric modulation of interactions [95, 96], in which the noise triggers the population of Bogoliubov modes according to the wave number selection or parametric resonance condition: $\epsilon(k) = \hbar\omega_m$. The Bogoliubov spectrum of a 2D homogeneous condensate is $\epsilon(k) = \sqrt{E_k\,(E_k + 2g_{2D}n_0)}$, where $E_k = \hbar^2k^2/2m$ with k being the quasi-momentum. For sufficiently small values of V_0 and large values of d we can still fairly approximate the spectrum of the trapped case with that of the homogeneous one using LDA for $k > 2\pi/R_{x,y}$. This low momenta cutoff introduces a low-frequency limit for the modulation frequency to observe pattern formation. Also, it has to be less than ω_z to preserve the 2D nature of the condensate.

Noise free:- With out noise, the Faraday patterns are not observed with the periodic modulation of the g_{2D}. Even for small V_0 we observe the formation of 2D DSs. In contrary to the linear quench, for the periodic case the depth of the gray soliton increases as a function of time and also the DSs are created continuously from the centre of the condensate. As a result, a transient 1D lattice of 2D DSs is formed after sufficiently long time, with the lattice periodicity depends on ω_m. Later, the lattice melts due to the SI. Note that, due to the inhomogeneity in the density, the periodicity at the centre is different from that of the edges of the condensate. The lattice periodicity, provided by the wavelength $\delta\lambda$, calculated at the centre, as a function of ω_m for different V_0 is shown in Fig. 9. Interestingly, the behaviour of $\delta\lambda$, is found to be very close to the wave number corresponding to the Bogoliubov frequency ω_m (dashed lines in Fig. 9) of the condensate at $V_0 = 0$. This indicates that, identical to the case of Faraday patterns, there is a wave number selection for DS lattice, closely connected to the Bogoliubov spectrum of the unmodulated condensate.

With noise:- The presence of noise leads to an interesting scenario where the soliton formation and Faraday patterns coexist, depending on V_0. In the absence of the potential barrier ($V0 = 0$) the Faraday patterns are seen as the result of parametric modulation of g_{2D}, see Fig. 10(a). For small, and nonzero V_0, the pattern, and DS lattice co-exist, see Fig. 10(b). Note that, the presence of pattern reduces the *darkness* of the DSs. For large V_0 we see the formation of a pattern-free DS lattice [see Fig. 10(c)], which eventually undergoes snake instability and breaks up into a gas of VDs. With large V_0, the soliton formation is enhanced, resulting in the fast formation of the lattice, which suppresses the pattern formation in the condensate.

Finally, we want to comment that similar results can be obtained by making either the potential barrier or the trapping frequency become time dependent instead of interactions.

V. CONCLUSION

In conclusion, we numerically analyzed the long-time dynamics of SI of 2D DSs in a TF condensate of rubidium atoms, with contact interactions. The DS is dynamically generated in the BEC by an initially imprinted phase gradient. The soliton properties as well as the nature of SI and post-instability dynamics depend substantially on the spatial width of the phase gradient. The VDs emerging from the unstable DS exhibits interesting dynamics such as the formation of vortexoniums, vortex annihilation, and exchange processes. The effective decay in the number of vortices is indirectly influenced by the spatial extension of the phase gradient. Alternative techniques for the DS generation, based on time-dependent interactions and an external Gaussian barrier are discussed. For the linear variation of interactions, the properties of the DS can be controlled by quench time. A transient DS lattice emerged in

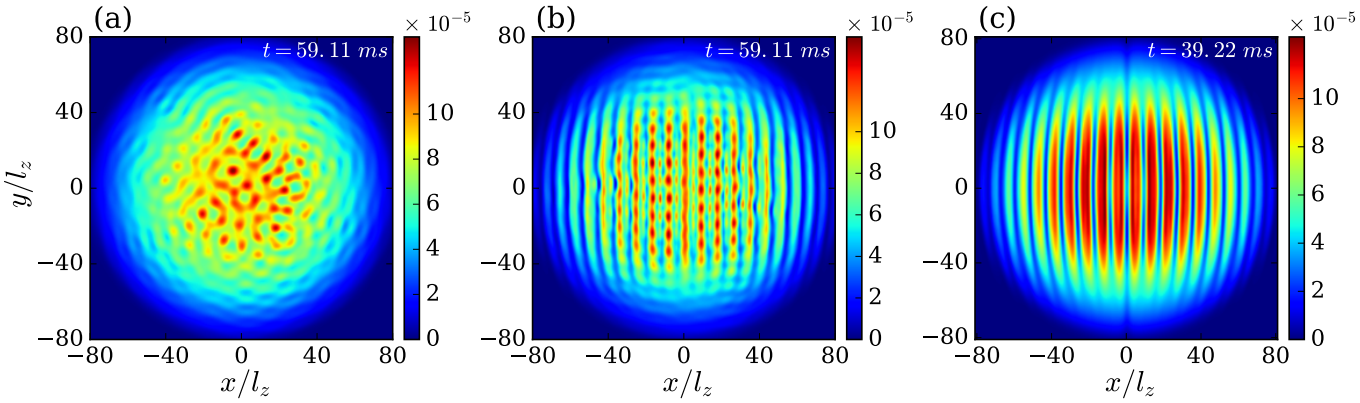


Figure 10. (a) Faraday patterns for $V_0 = 0$. (b) Co-existence of Faraday patterns and 2D DSs for $V_0 = 0.003\hbar\omega_z$. (c) Formation of pattern-free, transient DS lattice for $V_0 = 0.1\hbar\omega_z$. For all plots $\alpha = 0.2$ and $\omega_m = 0.6\omega_z$. The BEC setup is same as that of the Fig. 1.

the condensate for the parametric modulation of interactions, with lattice periodicity depending on the frequency of modulation. Interestingly, the scenario is richer by the co-existence of Faraday patterns and the transient DS lattice together. We also provide other techniques to generate DSs, which would provide similar results.

VI. ACKNOWLEDGMENTS

UDR would like to thank the Department of Science and Technology, Govt. of India through grants from EMR/2014/000365 and Nano Mission. R.N. acknowledges funding by the Indo-French Centre for the Promotion of Advanced Research.

[1] Y. S. Kivshar and B. Luther-Davies, Physics Reports **298**, 81 (1998).
[2] D. Krökel, N. J. Halas, G. Giuliani, and D. Grischkowsky, Phys. Rev. Lett. **60**, 29 (1988).
[3] G. A. Swartzlander, D. R. Andersen, J. J. Regan, H. Yin, and A. E. Kaplan, Phys. Rev. Lett. **66**, 1583 (1991).
[4] B. Denardo, W. Wright, S. Putterman, and A. Larraza, Phys. Rev. Lett. **64**, 1518 (1990).
[5] B. Denardo, B. Galvin, A. Greenfield, A. Larraza, S. Putterman, and W. Wright, Phys. Rev. Lett. **68**, 1730 (1992).
[6] M. Chen, M. A. Tsankov, J. M. Nash, and C. E. Patton, Phys. Rev. Lett. **70**, 1707 (1993).
[7] R. Heidemann, S. Zhdanov, R. Sütterlin, H. M. Thomas, and G. E. Morfill, Phys. Rev. Lett. **102**, 135002 (2009).
[8] P. G. Kevrekidis, D. J. Frantzeskakis, and R. Carretero-González, *Emergent nonlinear phenomena in Bose-Einstein condensates* (Springer, 2008).
[9] D. J. Frantzeskakis, Journal of Physics A: Mathematical and Theoretical **43**, 213001 (2010).
[10] P. G. Kevrekidis, D. J. Frantzeskakis, and R. Carretero-González, *The Defocusing Nonlinear Schrödinger equation* (Society for Industrial and applied mathematics, 2015).
[11] S. Burger, K. Bongs, S. Dettmer, W. Ertmer, K. Sengstock, A. Sanpera, G. V. Shlyapnikov, and M. Lewenstein, Phys. Rev. Lett. **83**, 5198 (1999).
[12] J. Denschlag, J. E. Simsarian, D. L. Feder, C. W. Clark, L. A. Collins, J. Cubizolles, L. Deng, E. W. Hagley, K. Helmerson, W. P. Reinhardt, et al., Science **287**, 97 (2000), ISSN 0036-8075.
[13] S. Stellmer, C. Becker, P. Soltan-Panahi, E.-M. Richter, S. Dörscher, M. Baumert, J. Kronjäger, K. Bongs, and K. Sengstock, Phys. Rev. Lett. **101**, 120406 (2008).
[14] H. Proud, M. Perea-Oritz, C. O'Neale, M. Baumert, M. Holynski, J. Kronjäger, G. Barontini, K. Bongs, and N. Meyer, arXiv:1609.08504 (2016).
[15] Z. Dutton, M. Budde, C. Slowe, and L. V. Hau, Science **293**, 663 (2001).
[16] J. J. Chang, P. Engels, and M. A. Hoefer, Phys. Rev. Lett. **101**, 170404 (2008).
[17] F. K. Abdullaev, A. M. Kamchatnov, V. V. Konotop, and V. A. Brazhnyi, Phys. Rev. Lett. **90**, 230402 (2003).
[18] L. D. Carr, J. Brand, S. Burger, and A. Sanpera, Phys. Rev. A **63**, 051601 (2001).
[19] S. Burger, L. D. Carr, P. Öhberg, K. Sengstock, and A. Sanpera, Phys. Rev. A **65**, 043611 (2002).
[20] B. P. Anderson, P. C. Haljan, C. A. Regal, D. L. Feder, L. A. Collins, C. W. Clark, and E. A. Cornell, Phys. Rev. Lett. **86**, 2926 (2001).
[21] C. Becker, S. Stellmer, P. Soltan-Panahi, S. Dorscher, M. Baumert, E.-M. Richter, J. Kronjager, K. Bongs, and K. Sengstock, Nat Phys **4**, 496 (2008).
[22] P. Engels and C. Atherton, Phys. Rev. Lett. **99**, 160405 (2007).
[23] I. Shomroni, E. Lahoud, S. Levy, and J. Steinhauer, Nat Phys **5**, 193 (2009).
[24] A. Weller, J. P. Ronzheimer, C. Gross, J. Esteve, M. K. Oberthaler, D. J. Frantzeskakis, G. Theocharis, and P. G. Kevrekidis, Phys. Rev. Lett. **101**, 130401 (2008).
[25] D. R. Scherer, C. N. Weiler, T. W. Neely, and B. P. Anderson, Phys. Rev. Lett. **98**, 110402 (2007).
[26] W. H. Zurek, Phys. Rev. Lett. **102**, 105702 (2009).
[27] G. Lamporesi, S. Donadello, S. Serafini, F. Dalfovo, and G. Ferrari, Nat Phys **9**, 656 (2013).
[28] B. Damski and W. H. Zurek, Phys. Rev. Lett. **104**, 160404 (2010).

[29] B. Wu, J. Liu, and Q. Niu, Phys. Rev. Lett. **88**, 034101 (2002).
[30] P. G. Kevrekidis, G. Theocharis, D. J. Frantzeskakis, and B. A. Malomed, Phys. Rev. Lett. **90**, 230401 (2003).
[31] D. Gallucci and N. P. Proukakis, New Journal of Physics **18**, 025004 (2016).
[32] G. Theocharis, P. Kevrekidis, H. Nistazakis, D. Frantzeskakis, and A. Bishop, Physics Letters A **337**, 441 (2005).
[33] G. Theocharis, P. Schmelcher, P. G. Kevrekidis, and D. J. Frantzeskakis, Phys. Rev. A **72**, 033614 (2005).
[34] A. Radouani, Phys. Rev. A **70**, 013602 (2004).
[35] A. D. Jackson, G. M. Kavoulakis, and C. J. Pethick, Phys. Rev. A **58**, 2417 (1998).
[36] A. E. Muryshev, H. B. van Linden van den Heuvell, and G. V. Shlyapnikov, Phys. Rev. A **60**, R2665 (1999).
[37] T. Busch and J. R. Anglin, Phys. Rev. Lett. **84**, 2298 (2000).
[38] L. D. Carr, C. W. Clark, and W. P. Reinhardt, Phys. Rev. A **62**, 063610 (2000).
[39] E. A. Kuznetsov and J. J. Rasmussen, Phys. Rev. E **51**, 4479 (1995).
[40] G. Huang, V. A. Makarov, and M. G. Velarde, Phys. Rev. A **67**, 023604 (2003).
[41] D. L. Feder, M. S. Pindzola, L. A. Collins, B. I. Schneider, and C. W. Clark, Phys. Rev. A **62**, 053606 (2000).
[42] B. P. Anderson, P. C. Haljan, C. A. Regal, D. L. Feder, L. A. Collins, C. W. Clark, and E. A. Cornell, Phys. Rev. Lett. **86**, 2926 (2001).
[43] V. Tikhonenko, J. Christou, B. Luther-Davies, and Y. S. Kivshar, Opt. Lett. **21**, 1129 (1996).
[44] A. V. Mamaev, M. Saffman, and A. A. Zozulya, Phys. Rev. Lett. **76**, 2262 (1996).
[45] A. Muryshev, G. V. Shlyapnikov, W. Ertmer, K. Sengstock, and M. Lewenstein, Phys. Rev. Lett. **89**, 110401 (2002).
[46] N. G. Parker, N. P. Proukakis, M. Leadbeater, and C. S. Adams, Phys. Rev. Lett. **90**, 220401 (2003).
[47] N. P. Proukakis, N. G. Parker, C. F. Barenghi, and C. S. Adams, Phys. Rev. Lett. **93**, 130408 (2004).
[48] D. E. Pelinovsky, D. J. Frantzeskakis, and P. G. Kevrekidis, Phys. Rev. E **72**, 016615 (2005).
[49] N. G. Parker, N. P. Proukakis, M. Leadbeater, and C. S. Adams, Journal of Physics B: Atomic, Molecular and Optical Physics **36**, 2891 (2003).
[50] B. A. Malomed, H. E. Nistazakis, D. J. Frantzeskakis, and P. G. Kevrekidis, Phys. Rev. A **70**, 043616 (2004).
[51] G. Huang, L. Deng, and C. Hang, Phys. Rev. E **72**, 036621 (2005).
[52] C. T. Law and G. A. Swartzlander, Opt. Lett. **18**, 586 (1993).
[53] G. McDonald, K. Syed, and W. Firth, Optics Communications **95**, 281 (1993), ISSN 0030-4018.
[54] Y. S. Kivshar and D. E. Pelinovsky, Physics Reports **331**, 117 (2000), ISSN 0370-1573.
[55] P. G. Kevrekidis, G. Theocharis, D. J. Frantzeskakis, and A. Trombettoni, Phys. Rev. A **70**, 023602 (2004).
[56] M. Ma, R. Carretero-González, P. G. Kevrekidis, D. J. Frantzeskakis, and B. A. Malomed, Phys. Rev. A **82**, 023621 (2010).
[57] L. A. Toikka and K.-A. Suominen, Phys. Rev. A **87**, 043601 (2013).
[58] A. Cetoli, J. Brand, R. G. Scott, F. Dalfovo, and L. P. Pitaevskii, Phys. Rev. A **88**, 043639 (2013).
[59] S. Middelkamp, P. G. Kevrekidis, D. J. Frantzeskakis, R. Carretero-González, and P. Schmelcher, Phys. Rev. A **82**, 013646 (2010).
[60] D. S. Rokhsar, Phys. Rev. Lett. **79**, 2164 (1997).
[61] E. J. M. Madarassy and C. F. Barenghi, Journal of Low Temperature Physics **152**, 122 (2008), ISSN 1573-7357.
[62] R. Navarro, R. Carretero-González, P. J. Torres, P. G. Kevrekidis, D. J. Frantzeskakis, M. W. Ray, E. Altuntaş, and D. S. Hall, Phys. Rev. Lett. **110**, 225301 (2013).
[63] L.-C. Crasovan, V. Vekslerchik, V. M. Pérez-García, J. P. Torres, D. Mihalache, and L. Torner, Phys. Rev. A **68**, 063609 (2003).
[64] Q. Zhou and H. Zhai, Phys. Rev. A **70**, 043619 (2004).
[65] M. Möttönen, S. M. M. Virtanen, T. Isoshima, and M. M. Salomaa, Phys. Rev. A **71**, 033626 (2005).
[66] V. Pietilä, M. Möttönen, T. Isoshima, J. A. M. Huhtamäki, and S. M. M. Virtanen, Phys. Rev. A **74**, 023603 (2006).
[67] A. Klein, D. Jaksch, Y. Zhang, and W. Bao, Phys. Rev. A **76**, 043602 (2007).
[68] W. Li, M. Haque, and S. Komineas, Phys. Rev. A **77**, 053610 (2008).
[69] D. V. Freilich, D. M. Bianchi, A. M. Kaufman, T. K. Langin, and D. S. Hall, Science **329**, 1182 (2010), ISSN 0036-8075.
[70] P. Torres, P. Kevrekidis, D. Frantzeskakis, R. Carretero-González, P. Schmelcher, and D. Hall, Physics Letters A **375**, 3044 (2011), ISSN 0375-9601.
[71] P. Kuopanportti, J. A. M. Huhtamäki, and M. Möttönen, Phys. Rev. A **83**, 011603 (2011).
[72] S. Middelkamp, P. J. Torres, P. G. Kevrekidis, D. J. Frantzeskakis, R. Carretero-González, P. Schmelcher, D. V. Freilich, and D. S. Hall, Phys. Rev. A **84**, 011605 (2011).
[73] T. W. Neely, E. C. Samson, A. S. Bradley, M. J. Davis, and B. P. Anderson, Phys. Rev. Lett. **104**, 160401 (2010).
[74] W. J. Kwon, S. W. Seo, and Y.-i. Shin, Phys. Rev. A **92**, 033613 (2015).
[75] R. H. Goodman, P. G. Kevrekidis, and R. Carretero-González, SIAM Journal on Applied Dynamical Systems **14**, 699 (2015).
[76] S. Prabhakar, R. P. Singh, S. Gautam, and D. Angom, Journal of Physics B: Atomic, Molecular and Optical Physics **46**, 125302 (2013).
[77] W. J. Kwon, G. Moon, J.-y. Choi, S. W. Seo, and Y.-i. Shin, Phys. Rev. A **90**, 063627 (2014).
[78] G. W. Stagg, A. J. Allen, N. G. Parker, and C. F. Barenghi, Phys. Rev. A **91**, 013612 (2015).
[79] Y. Du, C. Niu, Y. Tian, and H. Zhang, Journal of High Energy Physics **2015**, 18 (2015).
[80] C. Rorai, K. R. Sreenivasan, and M. E. Fisher, Phys. Rev. B **88**, 134522 (2013).
[81] T. Simula, M. J. Davis, and K. Helmerson, Phys. Rev. Lett. **113**, 165302 (2014).
[82] A. J. Groszek, T. P. Simula, D. M. Paganin, and K. Helmerson, Phys. Rev. A **93**, 043614 (2016).
[83] A. Görlitz, J. M. Vogels, A. E. Leanhardt, C. Raman, T. L. Gustavson, J. R. Abo-Shaeer, A. P. Chikkatur, S. Gupta, S. Inouye, T. Rosenband, et al., Phys. Rev. Lett. **87**, 130402 (2001).
[84] W. P. Reinhardt and S. B. McKinney, Physica Scripta **2001**, 202 (2001).
[85] V. V. Konotop and V. E. Vekslerchik, Journal of Physics A: Mathematical and General **24**, 767 (1991).
[86] V. V. Konotop and L. Pitaevskii, Phys. Rev. Lett. **93**, 240403 (2004).
[87] V. A. Brazhnyi, V. V. Konotop, and L. P. Pitaevskii, Phys. Rev. A **73**, 053601 (2006).
[88] L. A. Smirnov and A. I. Smirnov, Phys. Rev. A **92**, 013636 (2015).
[89] N. Parker, Ph.D. thesis, University of Durham (2004).
[90] C. Lee, E. A. Ostrovskaya, and Y. S. Kivshar, Journal of Physics B: Atomic, Molecular and Optical Physics **40**, 4235 (2007).

[91] T. F. Scott, R. J. Ballagh, and K. Burnett, Journal of Physics B: Atomic, Molecular and Optical Physics **31**, L329 (1998).

[92] S. E. Pollack, D. Dries, R. G. Hulet, K. M. F. Magalhães, E. A. L. Henn, E. R. F. Ramos, M. A. Caracanhas, and V. S. Bagnato, Phys. Rev. A **81**, 053627 (2010).

[93] H. Pu, P. Maenner, W. Zhang, and H. Y. Ling, Phys. Rev. Lett. **98**, 050406 (2007).

[94] Y. B. Band, B. Malomed, and M. Trippenbach, Phys. Rev. A **65**, 033607 (2002).

[95] K. Staliunas, S. Longhi, and G. J. de Valcárcel, Phys. Rev. Lett. **89**, 210406 (2002).

[96] P. Engels, C. Atherton, and M. A. Hoefer, Phys. Rev. Lett. **98**, 095301 (2007).